PAPER

Development of over-MW gyrotrons for fusion at 14 GHz to sub-THz frequencies

IOP Publishing | International Atomic Energy Agency Nuclear Fusion

Nucl. Fusion **57** (2017) 066001 (9pp) https://doi.org/10.1088/1741-4326/aa6875

Development of over-MW gyrotrons for fusion at 14 GHz to sub-THz frequencies

T. Kariya[1], T. Imai[1], R. Minami[1], K. Sakamoto[2], Y. Oda[2], R. Ikeda[2], T. Shimozuma[3], S. Kubo[3], H. Idei[4], T. Numakura[1], K. Tsumura[1], Y. Ebashi[1], M. Okada[1], Y. Nakashima[1], Y. Yoshimura[3], H. Takahashi[3], S. Ito[3], K. Hanada[4], K. Nagasaki[5], M. Ono[6], T. Eguchi[7] and Y. Mitsunaka[7]

[1] Plasma Research Center, University of Tsukuba, Ibaraki, Japan
[2] National Institutes for Quantum and Radiological Science and Technology, Ibaraki, Japan
[3] National Institute for Fusion Science, Gifu, Japan
[4] Research Institute for Applied Mechanics, Kyushu University, Fukuoka, Japan
[5] Institute of Advanced Energy, Kyoto University, Kyoto, Japan
[6] Princeton University Plasma Physics Laboratory, Princeton, NJ, United States of America
[7] Toshiba Electron Tubes and Devices Co., Ltd, Tochigi, Japan

E-mail: kariya@prc.tsukuba.ac.jp

Received 14 December 2016, revised 1 March 2017
Accepted for publication 22 March 2017
Published 11 April 2017

Abstract

Megawatt power gyrotrons are being developed for collaborative electron cyclotron heating (ECH) studies of advanced fusion devices and demonstration power plant (DEMO). (1) In the first experiment of a 300 GHz gyrotron, an output power above 0.5 MW in the $TE_{32,18}$ single mode was achieved with a pulse width of 2 ms. This was the first observation of MW-scale oscillations in a DEMO-relevant gyrotron mode. It was also found that the reflection at the output window affected the determination of the oscillation mode. Furthermore, several single mode oscillations in the 226–254 GHz range were confirmed, which is important for the step-frequency tunable gyrotron in the sub-THz frequency range. (2) Based on the successful results of the 77 and 154 GHz large helical device (LHD) tubes, a new 154/116 GHz dual-frequency gyrotron with an output of over 1.5 MW is being designed. (3) A new record output of 1.38 MW was obtained using an existing 28 GHz gyrotron. A newly designed tube aimed at achieving a dual-frequency output power of 2 MW at 28 GHz (0.4 MW continuous wave) and 1 MW at 35 GHz was built. In the first experimental test, main mode oscillations were observed at the frequencies of 28.036 and 34.831 GHz with Gaussian-like output beams and output power of 1.27 and 0.48 MW, respectively. A total efficiency of 50% was achieved at 28 GHz operation.

Keywords: gyrotron, ECH, ECCD

(Some figures may appear in colour only in the online journal)

1. Introduction

Electron cyclotron heating (ECH), electron cyclotron current drive (ECCD), and electron Bernstein wave (EBW) heating are attractive and promising schemes for achieving heating, current drive, and plasma control of fusion magnetic confinement systems, especially in future applications requiring dense and large-core plasma control. A gyrotron is a powerful and essential tool for achieving ECH, ECCD and EBW heating. At the Plasma Research Center (PRC) of the University of Tsukuba, megawatt (MW)-power gyrotrons, covering a wide range of frequencies (14–300 GHz), are being developed for existing fusion devices and future demonstration power plant (DEMO) in collaboration with several research organizations and universities [1, 2]. The most important element of our study is its contribution to nuclear fusion by the application

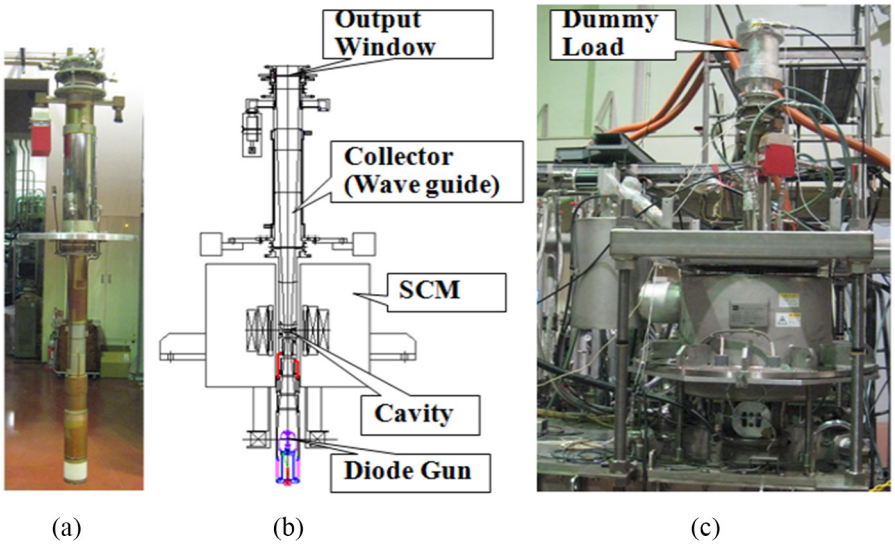

Figure 1. (*a*) Photograph of the 300 GHz gyrotron, (*b*) structural cross-section of the 300 GHz gyrotron, and (*c*) photograph of the oscillation test setup.

of these newly developed gyrotrons to plasma experiments. This contribution is expected to provide positive feedback to gyrotron collaborative projects.

The development of a 300 GHz gyrotron for ECH and ECCD on the DEMO is in progress in collaboration with National Institutes for Quantum and Radiological Science and Technology (QST). In the first experimental test, an output power of the order of hundreds of kilowatts was achieved with millisecond duration pulses [1, 3].

The joint program of National Institute for Fusion Science (NIFS) and the University of Tsukuba developed three 77 GHz and two 154 GHz gyrotrons for large helical device (LHD). Typically, the 77 GHz gyrotorns achieved a maximum output power of 1.9 MW and a quasi-CW (continuous wave) 75 min-long operation at 0.22 MW. The 154 GHz gyrotrons achieved a maximum output power of 1.25 MW and 30 min-long operation at 0.35 MW. A total plasma injection power of 5.4 MW was achieved using these gyrotrons. Gyrotrons have contributed to the enhancement of the LHD plasma performance in recent electron internal transport barrier (ITB) experiments. By combining high power ECH and neutral beam injection (NBI), high temperature plasmas with simultaneous high electron temperature (7–9 keV) and ion temperature (4–6 keV) have been obtained. A steady-state plasma with a line-averaged electron density of 1×10^{19} m^{-3} and electron temperature of 3.5 keV was sustained for 330 s. For the next step of NIFS gyrotron, a design study has commenced for 154 and 116 GHz dual-frequency gyrotron [4–7].

Currently, ECH physics experiments in some plasma devices require gyrotrons with a relatively low frequency (14–35 GHz). Furthermore, gyrotrons operating in this frequency range were used in a recent EBW experiment [8, 9]. For example, the Q-shu University Experiments with Steady-State Spherical Tokamak (QUEST), conducted at Kyushu University, require a 28 GHz 0.4 MW CW gyrotron. The collaboration between the University of Tsukuba and Kyushu University adapted Tsukuba's 28 GHz 1 MW gyrotron for use with the QUEST ECH system and demonstrated plasma heating and current drive effects. Successful results were obtained in the first QUEST plasma experiment using a 28 GHz gyrotron. Over-dense plasma with a density in excess of 1×10^{18} m^{-3} (higher than the cut-off density of 8.2 GHz) was produced. An EC-driven plasma current of 66 kA was achieved non-inductively for a 28 GHz injection [10]. Considering the above test results and future requirements, a new 28 and 35 GHz dual-frequency gyrotron is being developed. Achieving 35 GHz oscillations in the 28 GHz gyrotron would be very useful for collaborative research including applications to the National Spherical Torus Experiment (NSTX-U) of the Princeton Plasma Physics Laboratory (PPPL) [11] and the Helical-Axis Heliotron (Heliotron J) of Kyoto University. In the 100 GHz range, dual- or multi-frequency MW gyrotrons are being developed in many facilities for the purpose of nuclear fusion [12–17]. However, the development of dual-frequency gyrotrons at lower frequencies presents new challenges that are different from those encountered at higher frequencies.

In this paper, section 2 describes the recent test results of 300 GHz gyrotron. The design of a new 154/116 GHz dual-frequency gyrotron is discussed in section 3. The design and first experimental results of the new 28/35 GHz dual-frequency gyrotron are presented in section 4. discussion and conclusions are provided in sections 5 and 6, respectively.

2. Development of the sub-terahertz gyrotron

In collaboration with QST, the 300 GHz gyrotron was tested at the Tsukuba gyrotron test stand. Figure 1 shows (a) a photograph of the 300 GHz gyrotron, (b) a structural cross-section view, and (c) a photograph of oscillation test setup. This gyrotron is a conventional type without a built-in mode converter. The design cavity oscillation mode $TE_{32,18}$ is a very high mode to operate with MW-level power and long pulse. The electron gun is a diode gun, the output window is a single disk sapphire

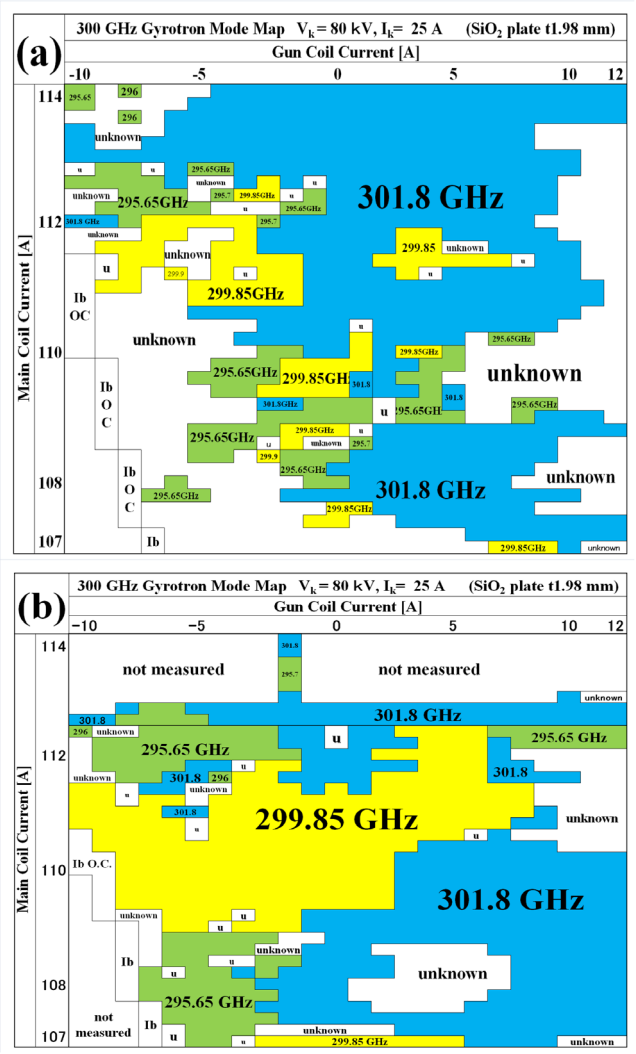

Figure 2. Oscillation mode map of 300 GHz gyrotron showing the cavity coil current and gun coil current (*a*) without an additional SiO_2 disk and (*b*) with an additional 1.98 mm-thick SiO_2 disk. The output window is an edge-cooled single-disk window with a 2.79 mm-thick sapphire disk.

window with a thickness of 2.79 mm and the overall length of the gyrotron is 1987 mm. A superconducting magnet (SCM) with a bore diameter of 110 mm produces a strong 13 T magnetic field. The output power was measured calorimetrically by using a SiC dummy load. Using a spectrum analyzer, oscillation frequencies of 300, 296, and 302 GHz were measured first. Based on these measurement results, the oscillation frequencies were determined with a heterodyne detection system using a 22nd harmonic mixer [3]. The output RF signal was converted to an IF signal in the DC—2.5 GHz range using a mixer. The IF signal was provided to three mode detection channels with a detector and band-pass filter corresponding to each oscillation mode. The mode number m and the rotation direction of the $TE_{m,n}$ mode were confirmed by the burn pattern of the output RF at the output window. The smallest radius with the strongest burn pattern was compared with the calculated radius of the first peak of the $TE_{m,n}$ mode.

It was observed that the RF reflection at the output window affected the cavity oscillations so that the competing mode

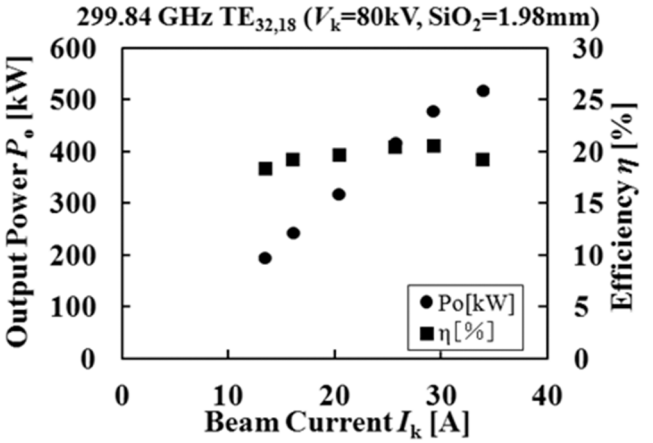

Figure 3. Dependence of the output power and output efficiency on the beam current for 299.84 GHz oscillations.

$TE_{30,19}$ oscillated more strongly than the main mode $TE_{32,18}$. Figures 2(*a*) and (*b*) show the mode maps (magnetic field at the cavity versus the field at the gun) obtained with and without a SiO_2 disk attached to the output window, respectively. Without a SiO_2 disk, the calculated reflectance was 0% for $TE_{32,18}$ and 23% for $TE_{30,19}$. With a SiO_2 disk of 1.98 mm thickness, the calculated reflectance was 20% for $TE_{32,18}$ and 2% for $TE_{30,19}$. For $TE_{32,18}$, the oscillation region was expanded in the mode map by adjusting the window reflection. A $TE_{m,n}$ mode RF reflected at the window returned to the cavity as a $TE_{m,n}$ mode. Therefore, the effective Q value of the cavity for the competing mode, which had a larger window reflection, increased. This facilitated the competing mode oscillation.

The dependences of the output power and efficiency of the $TE_{32,18}$ (299.84 GHz) oscillation on the beam current are shown in figure 3. An output power of 522 kW was achieved with a pulse width of 2 ms. Similarly, output powers of 542 kW for 295.65 GHz ($TE_{31,18}$) and 528 kW for 301.8 GHz ($TE_{30,19}$) were obtained.

Furthermore, investigations of oscillations were conducted for a frequency of approximately 240 GHz. When the cavity and gun coil currents were swept within the operating range, seven output power peaks of approximately 300 kW were observed. The radial mode number m, the smallest peak power radius, and the rotation direction of the output RF were measured using the burn patterns at the output window. The injection radius of the electron beam was calculated from the cavity and gun coil currents. The oscillation modes and their frequencies were estimated by ensuring that the experimental and calculated results were consistent with each other. The characteristics of the estimated modes are listed in table 1. The oscillations were observed for frequencies in the 226–254 GHz range. This is critical for obtaining the single pure-mode oscillation at each step frequency in the sub-THz region.

In the next stage of the development of the DEMO subterahertz gyrotron, the impact of the window reflection will be removed by installing a built-in mode converter. This is because a mode converter cannot radiate a counter-rotating mode as a Gaussian beam or the cavity oscillation mode at a different radiation angle at the mode converter cannot return to the cavity as a circular waveguide mode. The electron beam

Table 1. Estimations of the oscillation modes and frequencies from the 220–240 GHz oscillation test results.

220–240 GHz oscillation by 300 GHz gyrotron ($V_k = 70$ kV, $I_k = 21.6$ A, 2 ms)				
Magnetic field at cavity (T)	Beam radius (mm)	Estimated oscillation mode	Estimated frequency (GHz)	Output power (kW)
10.11	5.57	$TE^{(-)}_{28,15}$	253.99	310
9.80	5.58	$TE^{(-)}_{27,15}$	250.04	292
9.60	5.59	$TE^{(-)}_{28,14}$	243.9	345
9.54	5.59	$TE^{(+)}_{25,15}$	242.1	288
9.43	5.6	?	?	
9.07	5.61	$TE^{(+)}_{24,14}$	228.13	285
8.90	5.62	$TE^{(-)}_{26,13}$	225.96	274

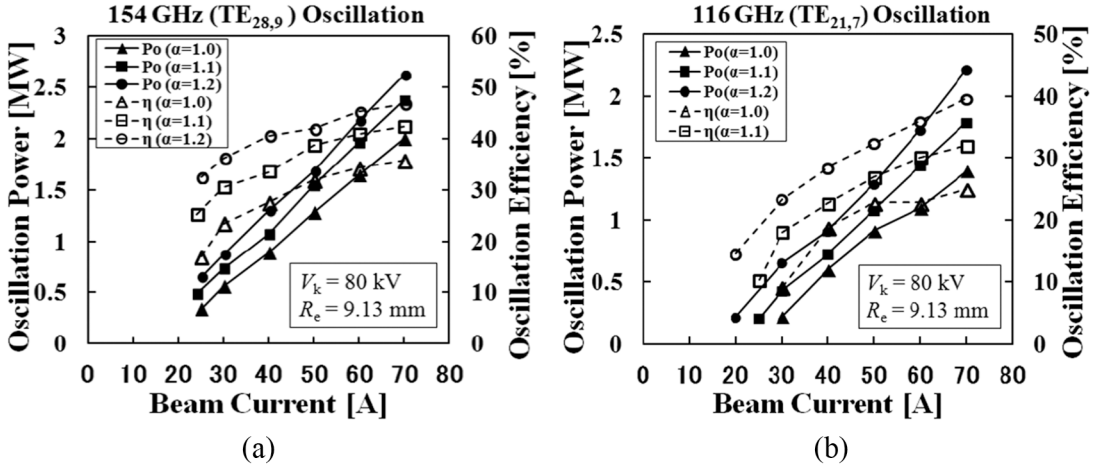

Figure 4. Calculated dependence of the cavity oscillation power on the beam current at (*a*) 154 GHz and (*b*) 116 GHz.

parameters can be controlled using a triode gun instead of a diode gun, which might increase the output power. Using a diamond window provides a wide frequency bandwidth and enables the operation of the device at higher power and with longer-duration pulses.

3. Development of the 154/116 GHz gyrotron

A design study of the new 154/116 GHz dual-frequency gyrotron has been started to expand the range of the LHD plasma parameters. The combination of cavity oscillation modes for the two frequencies must be able to exist in the same cavity structure. The difference between the radiation angles of the $f_1 = 154$ GHz and $f_2 = 116$ GHz cavity modes must be almost 0° to achieve a high RF beam transmission efficiency for both modes using the same internal mirrors. In addition, under the magnetic field distribution produced by the SCM, a magnetron injection gun (MIG) is required to inject the electron beam at the first peak of the cavity electric field for both oscillation modes with a pitch factor $\alpha = 1.0$–1.2. We selected the following combination of cavity oscillation modes: $TE_{28,9}$ with $f_1 = 154$ GHz and $TE_{21,7}$ with $f_2 = 116$ GHz. The calculated dependence of the cavity oscillation power on the beam current at 154 and 116 GHz is shown in figure 4. For both frequencies, oscillations above 1.5 MW are expected with an electron beam pitch factor $\alpha = 1$ for a beam voltage $V_k = 80$ kV, beam current $I_k = 70$ A and electron beam radius $R_e = 9.13$ mm. The calculated heat loads of the cavity inner wall for 1.5 MW oscillations are 1.5 kW cm^{-2} at 154 GHz and 0.8 kW cm^{-2} at 116 GHz. The design of the triode MIG is the same as that used in the 77 GHz and 154 GHz gyrotrons, which is advantageous for fabrication. From the dependences of the pitch factor α and its spread $\Delta\alpha/\alpha$ on the anode voltage, the MIG is expected to operate in both the 154 and 116 GHz frequencies with $\alpha = 1$–1.2 and $\Delta\alpha/\alpha < 5$ % at $V_k = 80$ kV and $I_k = 60$ A, indicating high efficient oscillations in the cavity. The mode converter was optimized for both the 154 GHz $TE_{28,9}$ and 116 GHz $TE_{21,7}$ modes using the electric field integral equation code SURF3D [18]. Using a system of four elliptical mirrors (without phase-correcting mirrors with non-quadratic surface contour function), the RF beam radiated from the mode converter is focused and transmitted to the outside of the tube through the output window. The calculated RF beam at the output window has a clear Gaussian beam profile at both 154 and 116 GHz. The total calculated transmission efficiencies at the output window are 97.8% for 154 GHz and 98.1% for 116 GHz. The designs of the mode converter and the mirrors will be improved to obtain higher efficiencies at both frequencies. The reflectance of the diamond window is 0% at 154 GHz and 0.2% at 116 GHz. The collector (inner diameter of 320 mm) has sweep coils to reduce its heat load, which is caused by the spent electron beam. For $V_k = 80$ kV, $I_k = 70$ A, $V_{cpd} = 25$ kV (defined in section 4.1), and $\eta_o = 35\%$, the spent beam energy is approximately 2.8 MW. The axial distributions

Table 2. Design parameters of the 28/35 GHz dual-frequency gyrotron.

28 GHz 2 MW dual-frequency gyrotron			
Frequency	28 GHz		34.77 GHz
Output power	2 MW	0.4 MW	1 MW
Pulse width	3 s	CW	3 s
Output efficiency	50% (with CPD)		
Beam voltage	80 kV	70 kV	80 kV
Beam current	70 A	20 A	40 A
MIG	Triode		
Cavity mode	$TE_{8,5}$		$TE_{10,6}$
Output mode	Gaussian like		
Output window	Sapphire double disk		
Collector	Depressed collector		
	Sweeping coils		

of the average deposition power density on the collector were calculated. The peak average deposition power densities for both frequencies were below 0.6 kW cm^{-2} with a spent beam power of 2.8 MW. This deposition power density is in the same level as that of the ITER 170 GHz gyrotron. These results indicate that the collector can operate at 1 MW CW.

4. Development of the 28/35 GHz dual-frequency gyrotron

A 28 GHz 1 MW gyrotron developed for GAMMA 10/PDX achieved an output power of 1.38 MW in a 2015 experiment after improving the power supply. This gyrotron achieved stable operation at 0.6 MW for 2 s for $V_k = 70$ kV and $I_k = 23.9$ A. The output power and pulse width were limited by the power supply and the water dummy load. After reinstalling this gyrotron, the QUEST plasma experiment using the 28 GHz gyrotron was resumed, and an EC-driven plasma current of 70 kA was achieved non-inductively with a 120 kW power injection by a new movable launcher system [19]. In addition to this collaborative research project, a new 28/35 GHz dual-frequency gyrotron is being developed for GAMMA 10/PDX, QUEST, NSTX-U and Heliotron J.

4.1. Specification of the dual-frequency gyrotron

The design targets for the 28/35 GHz dual-frequency gyrotron are listed in table 2, and its structural cross section is shown in figure 5(*a*). The power targets at 28 GHz are 2 MW for 3 s pulse duration and a 0.4 MW CW, whereas the power target at 35 GHz is 1 MW for 3 s. A triode MIG is used to control the electron beam parameters by varying the anode voltage. Combination of cavity oscillation modes in the $TE_{8,5}$ mode for 28 GHz and in the $TE_{10,6}$ mode for 34.8 GHz was chosen by considering the oscillation frequency, the radiation angle of the mode converter, the frequency matching of the output window, and the electron beam trajectories for both modes. According to the cavity simulation results, 28 GHz oscillations with a power greater than 2 MW are expected for $I_k = 70$ A with $\alpha > 1$. In the same cavity structure, 34.8 GHz oscillations with a power greater than 1 MW were obtained for

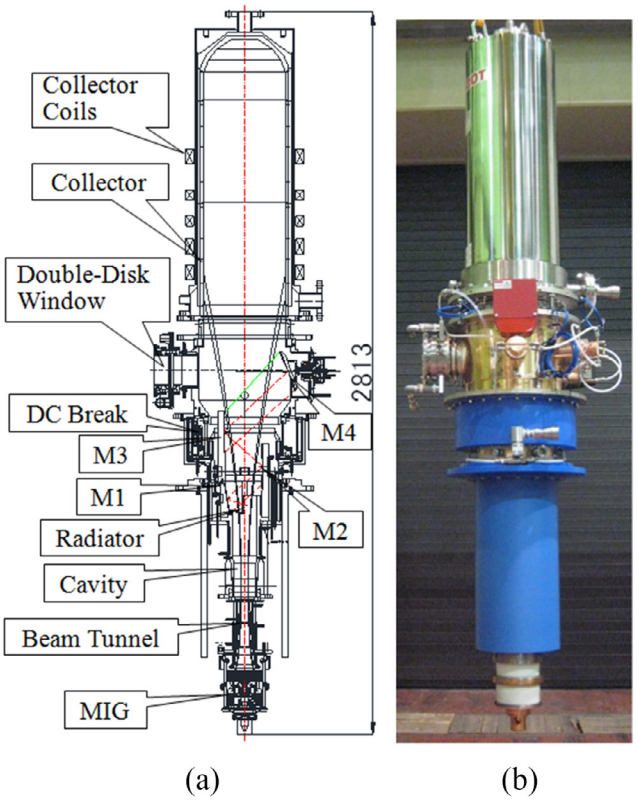

Figure 5. (*a*) Structural cross-section and (*b*) photograph of the 28/35 GHz dual-frequency gyrotron.

$I_k = 40$ A with $\alpha > 1$. The calculated results show that these designs can achieve the target output power for the 28/35 GHz dual-frequency gyrotron. The RF wave will be converted to a Gaussian-like beam by a built-in quasi-optical mode converter and will be then transmitted by a system of four mirrors to the outside of the tube through an output window. The total transmission efficiency from the mode converter to the output window was calculated to be 97.4% at 28 GHz and 97.0% at 34.77 GHz. The profile and the phase of the output RF beam will be adjusted using a matching optics unit (MOU), and the beam will be coupled to a corrugated waveguide in the HE_{11} mode. The calculated total transmission efficiency from the mode converter to the corrugated waveguide is 96.2% at 28 GHz and 96.4% at 34.77 GHz. The output window is a sapphire double-disk window (disk thickness 6.98 mm and gap length 4 mm) cooled with a fluorocarbon coolant (FC-3283). The dielectric constant and loss tangent of FC-3283 were measured with a Fabry–Pérot cavity to be 1.87 and 2.5×10^{-3}, respectively. The calculation results for the output window indicate that both targets (2 MW 3 s and 0.4 MW CW) were met at 28 GHz and that a 3 s 1 MW operation was possible at 34.8 GHz. The collector utilizes a collector potential depression (CPD) for efficiency enhancement and has sweep coils to reduce its heat load. The efficiency is enhanced by a factor of V_k/V_M, i.e. the total efficiency with CPD is $\eta_{cpd} = \eta_o V_k/V_M$. Here, $V_M (= V_k - V_{cpd})$ and V_{cpd} are the main power supply and CPD voltages, respectively. The CPD voltage is the beam deceleration voltage supplied between the body section (including beam tunnel, cavity, mode converter, and mirrors)

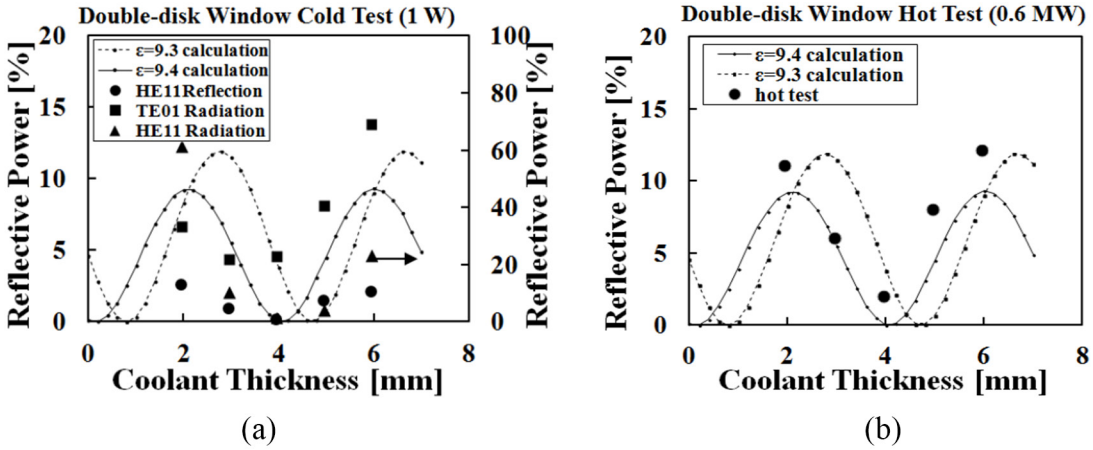

Figure 6. Dependence of the reflective power of the double-disk window on the coolant thickness using (*a*) a Gunn diode oscillator power (1 W) and (*b*) gyrotron power (600 kW). The solid and dashed curves represent the calculated reflectance with $\varepsilon = 9.4$ and 9.3, respectively.

and the collector, and η_o is the output efficiency. The peak average deposition power density of the collector was below 0.54 kW cm^{-2} with a spent beam power of 2.8 MW. These results suggest that the collector can function efficiently at 0.4 MW CW operation. The gyrotron has a DC-break section in order to sustain a high voltage between the body section and the (grounded) collector. Likewise, the gyrotron has a body insulation jacket to sustain the high voltage between the body section and the (grounded) SCM.

4.2. Preliminary test of the dual-frequency gyrotron output window

The dual-frequency gyrotron has a sapphire double-disk window that enables 0.4 MW CW operation. The frequency characteristics of the double-disk window depend on the thickness (depends on manufacturing accuracy) and permittivity (a function of the frequency) of the sapphire disk and fluorocarbon coolant (FC-3283, which is a substitute for FC-75). The frequency characteristics of the double-disk window can be adjusted by varying the thickness of the fluorocarbon coolant layer. Before installing the double-disk window in the dual-frequency gyrotron, we confirmed the dependence of its reflective power on the coolant thickness by performing a cold test using a Gunn diode oscillator with a power of 1 W and a hot test using a gyrotron output power of 600 kW. The results of these tests are shown in figures 6(*a*) and (*b*), respectively. The solid and dashed curves show the calculated reflectance for a sapphire dielectric constant of 9.4 and 9.3, respectively. In the cold test, the discrepancies between the calculations and the cold test results were due to the interference of the diverging incident or reflected waves. In the hot test, the reflective power was below 2% for a coolant layer thickness of approximately 4 mm. The calculated absorbed power of the double-disk window was under 1%. In addition, the uniform flow of the coolant on the sapphire surface was confirmed, which is important for achieving a high cooling efficiency. For the inlet and outlet structures of the coolant, a $6 \times 50\,\text{mm}^2$ rectangular structure yielded better results than a pipe structure with an inner diameter of 6 mm in terms of uniform flow and smaller pressure loss.

4.3. Experimental results for the dual-frequency gyrotron

The fabricated 28/35 GHz dual-frequency gyrotron is shown in figure 5(*b*). The new gyrotron was installed on the test stand of the University of Tsukuba. In the first 3 weeks testing phase, the main mode oscillations in the frequencies of 28.032–28.045 GHz were confirmed with a Gaussian-like beam. The output RF profile was measured form the burn patterns at the output window. The oscillation frequencies were measured using a cavity frequency meter. The thickness of the coolant layer on the double disk-window was fine-tuned to the maximum possible extent and the optimal coolant layer thickness was determined to be 4 mm, the same as that used in the preliminary test. The maximum output power of the double-disk window was 2% lower than that of a single disk window without the outer sapphire component and the coolant. This suggest that the reflection or power absorption of the double-disk window may be higher than the calculated result. The output power became unstable at a reflectance of approximately 10%, which suggests that the reflection from the window may affect the cavity oscillation [20]. Based on the comparison with the output power for the single-disk window, the reflectance of the double-disk window was approximately 0% at 34.82 GHz.

The dependences of the output power P_o and output efficiency η_o on I_k for $V_k = 80$ kV are shown in figure 7. The measurement of P_o was performed calorimetrically using the SiC water load at the output window. The magnetic field and anode voltage were optimized for different beam current values. An output power of 1.25 MW with a pulse duration of 2 mm was obtained at $I_k = 51.5$ A with $\eta_o = 30.8\%$. The gyrotron tests were performed using a direct current high voltage generator (DCG) in the present experiment. Because the DCG specifications were 70 kV and 50 A, V_k was unstable for $I_k > 51$ A.

The dependencies of the cavity magnetic field and anode voltage on the output power were measured at the output power of 1 MW. These characteristics were confirmed to be in their normal ranges.

The dependences of P_o, η_o, the total efficiency η_t (which includes the efficiency enhancement by the CPD), the anode

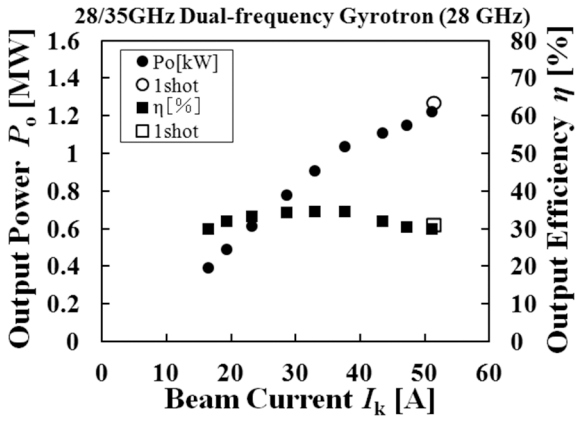

Figure 7. Dependence of the output power and efficiency on the beam current at a beam voltage of 80 kV in the 28 GHz oscillation test.

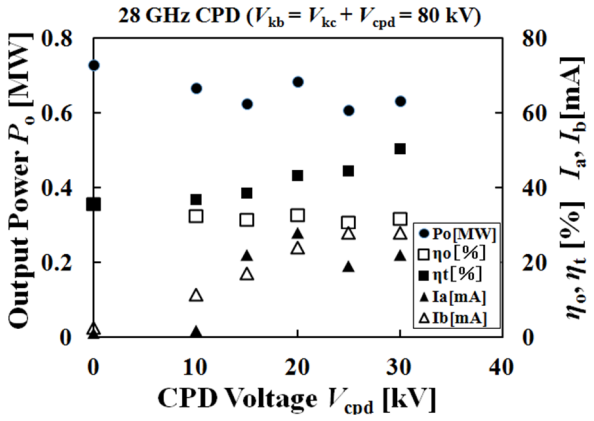

Figure 8. Dependence of output power, output efficiency, total efficiency (including the efficiency enhancement by CPD), anode current and body current, on the CPD voltage.

current I_a, and the body current I_b on V_{cpd} are shown in figure 8. The figure indicates that η_t increased with V_{cpd} achieving a maximum total efficiency of 50%. In contrast, P_o and η_o decreased with increasing V_{cpd} while I_a and I_b (which includes the leak current of the coolant water) increased with V_{cpd}, which was caused by the electrons reflected by V_{cpd}. This indicates that the α spread of the electron beam was not negligible.

The oscillation in the 34.8 GHz mode was observed at a frequency of 34.82 GHz with a Gaussian-like beam. The output beam position was at the center of the output window in the same position as that of the 28 GHz output beam. The design of the RF transmission system was confirmed to be correct. The output power and efficiency at a frequency of 34.8 GHz were 0.48 MW and 12.2%, respectively, for $V_k = 80$ kV and $I_k = 49.3$ A. The low output efficiency could be attributed to the low pitch factor of the electron beam, which impedes the increase of the anode voltage.

To measure the temperature characteristic of the output window, the gyrotron conditioning was progressed with a 0.7 MW power level for 700 ms. After suspending the conditioning for 3 weeks, the outer sapphire disk was damaged by the discharge at the pulse width of 70 ms. It is thought that the RF discharge was caused by the direct RF reflection from the dummy load. When operating the gyrotrons on the plasma heating experiment, we must consider the RF reflections from the RF transmission line or the plasma.

5. Discussion

In this section, we discuss the results obtained for the 28/35 GHz dual-frequency gyrotron compared with those of the previous 28 GHz 1 MW gyrotron. The 28 GHz 1 MW gyrotron is the first tube with over 1 MW developed in the University of Tsukuba and is currently being used in the QUEST ECH experiments. The dual-frequency gyrotron has identical MIG structure and beam injection radius at the cavity but uses a different cavity oscillation mode and has a cavity design optimized for dual-frequency oscillation and 2 MW output, as described in section 4.1.

Figures 9(*a*) and (*b*) show a comparison of the two gyrotrons in terms of the dependence of the beam current on the cathode heater power and that of the output power on the anode voltage V_{ak}, respectively. In figure 9(*b*), V_{ak} represents the values that obtained the maximum output power for each beam current. As shown in figure 9(*a*), the beam current of the dual-frequency gyrotron is higher than that of the 1 MW gyrotron for the same cathode heater power. This characteristic difference may be due to the cathode emission inhomogeneity. As shown in figure 9(*b*), the optimal V_{ak} values of the dual-frequency gyrotron are lower than those of the 1 MW gyrotron and this difference increases with increasing output power. This result suggests that the decrease of α and increase of the α spread of the dual-frequency gyrotron are higher than those of the 1 MW gyrotron in the high power operation region.

The dependences of the experimentally obtained and calculated output power on the beam current of the 28 GHz 1 MW gyrotron and the dual-frequency gyrotron (28 GHz oscillation) are shown in figures 10(*a*) and (*b*). The experimental output power was measured at the output window with $V_k = 80$ kV. The calculations were adjusted to determine the calculated window output power by multiplying the calculated cavity oscillation power with each pitch factor α by the calculated transmission efficiency from the mode converter to the window. The calculated transmission efficiency was 94.7% for the 1 MW gyrotron and 97.4% for the dual-frequency gyrotron at 28 GHz oscillation. The calculated power increased with the increase of α and I_k. The experimental output powers, shown by the closed circles, increased with the beam current I_k but tended to saturate at higher I_k. The comparison between the experimental and calculated results of the 1 MW gyrotron (figure 10(*a*)) shows that the electron beam can have $\alpha = 1.2$–1.3 at $I_k = 20$ A. The value of α appears to decrease with increasing I_k, and to become 1.0–1.1 at $I_k = 40$ A and approximately 1.0 at $I_k = 50$ A. The comparison between the experimental and calculated results of the dual-frequency gyrotron (figure 10(*b*)) shows that the electron beam appears to have $\alpha = 1.1$–1.2 at $I_k = 20$ A. The value of α appears to decrease with increasing I_k and to become approximately 1.0 at $I_k = 40$ A and 0.9–1.0 at $I_k = 50$ A. The α value of the dual-frequency gyrotron appears to be smaller than that of the 1 MW gyrotron. The MIG structure and the operation

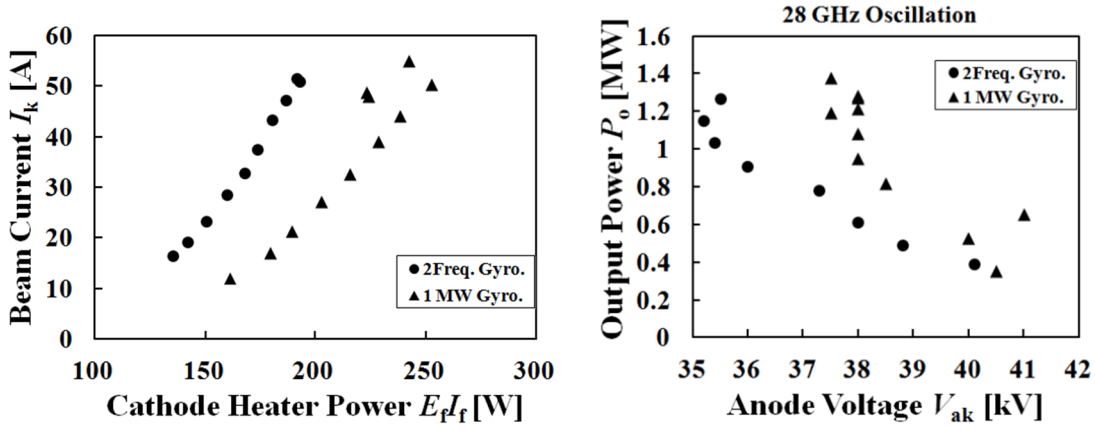

(a) (b)

Figure 9. Comparison between the operations of the 28 GHz 1 MW gyrotron and the dual-frequency gyrotron at 28 GHz. (*a*) Dependence of the beam current on the cathode heater power and (*b*) dependence of the output power on the anode voltage.

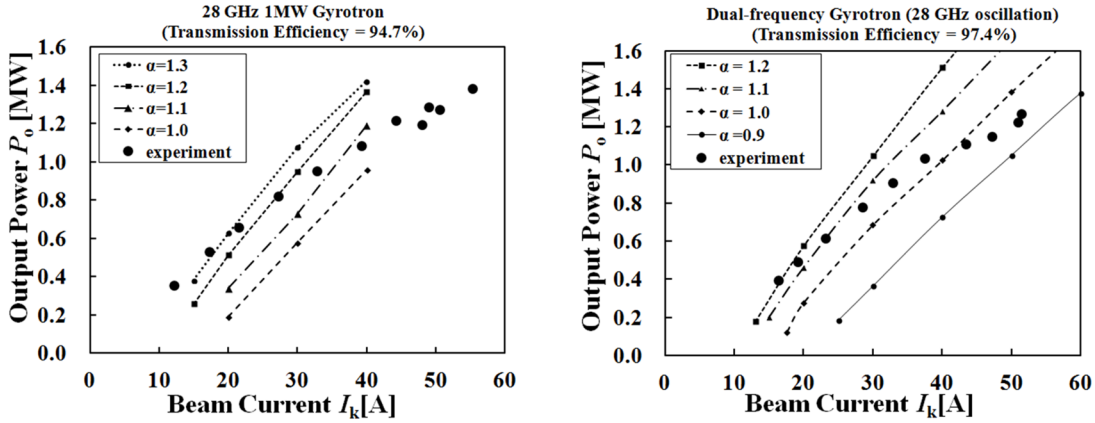

(a) (b)

Figure 10. Dependence of the experimental and calculated output power on the beam current for (*a*) the 28 GHz 1 MW gyrotron and (*b*) the dual-frequency gyrotron (28 GHz oscillation).

parameters of the anode voltage of the dual-frequency gyrotron were identical to those of the 28 GHz 1 MW gyrotron. Regarding the reasons for the difference between the α values of the two gyrotron, the following causes are considered: (1) the misalignment between the SCM and the gyrotron, (2) the influence of the plasma production caused by outgassing from the new inner wall of the gyrotron, or (3) the problems caused by the fabrication of the MIG (the alignment of the electrodes or the uniformity of the cathode emission belt). This tendency of α decrease and the α spread to increase, which reduces the efficiency or degrades the optimization of the operation parameters owing to the increase of I_a, is one of the issues encountered in the development of higher power and higher efficiency gyrotron.

6. Conclusions

A MW-power 300 GHz gyrotron is being developed for the DEMO. An output power exceeding 0.5 MW with a pulse width of 2 ms was achieved in the $TE_{32,18}$ single-mode, which was the first observation of MW-scale oscillations for a DEMO-relevant ECH gyrotron mode. In addition, the reflection at the output window was observed to affect the oscillation mode characteristics. However, this problem can be eliminated by appropriate measures. Similarly, output powers of over 500 kW were achieved at 295.65 GHz ($TE_{31,18}$) and 301.8 GHz ($TE_{30,19}$) and oscillations were obtained in the 226–254 GHz frequency range. These results are critical for the development of a step-frequency tunable gyrotron in the sub-THz region for the DEMO.

A design study of a new 154/116 GHz dual-frequency gyrotron has been launched to expand the range of the LHD plasma parameters. A combination of cavity oscillation modes was chosen in the $TE_{28,9}$ mode at 154 GHz and in the $TE_{21,7}$ mode at 116 GHz. Oscillations with a power exceeding 1.5 MW are expected with an electron beam pitch factor $\alpha = 1$ at a beam current of 70 A. Design studies of the MIG, mode converter, transmission mirrors, output window, and collector were performed.

A new 28/35 GHz dual-frequency gyrotron (2 MW 3 s and 0.4 MW CW operation) is being developed for QUEST, NSTX-U, Heliotron J and GAMMA 10/PDX. A preliminary test of a double-disk sapphire window was performed before installation in the gyrotron. The frequency characteristics of

the double-disk window were optimized, and the coolant flow was confirmed. The main mode oscillations were confirmed at the frequencies of 28.036 and 34.831 GHz with Gaussian-like beams and output powers of 1.27 and 0.48 MW, respectively. A total efficiency of 50% was achieved at 28 GHz operation.

Current development studies of gyrotrons are aimed at multi-MW power and CW operation in the wide frequency range from 14 GHz to sub-THz levels. The implementation of the newly developed gyrotrons in actual plasma devices is expected to enable the efficient performance of nuclear fusion studies.

Acknowledgments

This work was partially supported by the NIFS collaborative program (NIFS13KUGM080, NIFS16KUGM106, NIFS14KUGM095, NIFS14KUGM086, and COD27077) and the grant-in-aid for scientific research from the Ministry of Education, Science, Sports and Culture of Japan (15H05770A and 25249135, 26249141).

References

[1] Kariya T. *et al* 2015 *Nucl. Fusion* **55** 093009
[2] Imai T. *et al* 2010 *Proc. 23rd Int. Conf. on Fusion Energy (Daejeon, 2010)* (Vienna: IAEA) CD-ROM file [FTP/P6-12] (www-naweb.iaea.org/napc/physics/fec/fec2010/papers/ftp_p6-12.pdf)
[3] Oda Y. *et al* 2015 *40th Int. Conf. on Infrared, Millimeter and Teraherz Waves (Hong Kong, 2015)* TS-68 (http://ieeexplore.ieee.org/document/7327812/)
[4] Kariya T. *et al* 2009 *Trans. Fusion Sci. Technol.* **55** 91–4
[5] Takahashi H. *et al* 2010 *Trans. Fusion Sci. Technol.* **57** 19–6
[6] Minami R. *et al* 2013 *Nucl. Fusion* **53** 063003
[7] Takahashi H. *et al* 2014 *Phys. Plasmas* **21** 061506
[8] Idei H. *et al* 2012 *Plasma Fusion Res.* **7** 2402112
[9] Ikeda R. *et al* 2010 *Contrib. Plasma Phys.* **50** 567
[10] Idei H. *et al* 2014 Fully non-inductive current drive experiment using 28 GHz and 8.2 GHz electron cyclotron waves in QUEST, paper presented at *25th IAEA Int. Conf. on Fusion Energy* (*Saint Petersburg, Russia, 2014*) [EX/P1-38] (www-naweb.iaea.org/napc/physics/fec/fec2014/fec2014-preprints/216_EXP138.pdf)
[11] Taylor G. *et al* 2012 *Proc. 17th Joint Workshop on ECE and ECRH (Deurne, 7–10 May 2012)* EPJ Web vol 32 p 02014
[12] Tax D.S. *et al* 2014 *IEEE Trans. Plasma Sci.* **42** 1128–34
[13] Diwei L., Yang Y. and Shenggang L. 2012 *Fusion Eng. Des.* **87** 1533–5
[14] Litvak A.G. *et al* 2012 *Proc. 17th Joint Workshop on ECE and ECRH* EPJ Web vol 32 p 04003
[15] Kobayashi T. *et al* 2013 *Trans. Fusion Sci. Technol.* **63** 160–3
[16] Sakamoto K. *et al* 2009 *Nucl. Fusion* **49** 095019
[17] Sakamoto K. *et al* 2013 *IEEE 14th Int. Vacuum Electronics Conf.* (*Paris, France 2013*)
[18] Neilson J. and Bunger R. 2002 *IEEE Trans. Plasma Sci.* **30** 794
[19] Idei H. *et al* 2016 Non-inductive electron cyclotron heating and current drive with dual frequency (8.2 /28 GHz) waves in QUEST *Nucl. Fusion* submitted
[20] Dammertz G. *et al* 1999 *IEEE Trans. Plasma Sci.* **PS-27** 330–9